Journal of Nuclear Science and Technology

ISSN: 0022-3131 (Print) 1881-1248 (Online) Journal homepage: http://www.tandfonline.com/loi/tnst20

Evaluation of Neutron Cross Sections of Hydrogen from 20 MeV to 1 GeV

Satoshi CHIBA , Sin-ichi MORIOKA & Tokio FUKAHORI

To cite this article: Satoshi CHIBA , Sin-ichi MORIOKA & Tokio FUKAHORI (1996) Evaluation of Neutron Cross Sections of Hydrogen from 20 MeV to 1 GeV, Journal of Nuclear Science and Technology, 33:8, 654-662, DOI: 10.1080/18811248.1996.9731973

To link to this article: https://doi.org/10.1080/18811248.1996.9731973

Published online: 15 Mar 2012.

Journal of NUCLEAR SCIENCE and TECHNOLOGY, Vol. 33, No. 8, p. 654–662 (August 1996)

TECHNICAL REPORT

Evaluation of Neutron Cross Sections of Hydrogen from 20 MeV to 1 GeV

Satoshi CHIBA*,†, Sin-ichi MORIOKA** and Tokio FUKAHORI*

* *Tokai Research Establishment, Japan Atomic Energy Research Institute*
** *CRC Research Institute*

(Received April 5, 1996)

The neutron cross sections of hydrogen (^{1}H) have been evaluated in the energy region from 20 MeV to 1 GeV. Evaluated quantities are the total, elastic and inelastic scattering and capture cross sections, covariance matrix of total cross section and photon production cross section associated with the capture process. The total cross section was evaluated by combining the results obtained from the generalized least-squares method and the phase-shift data. The phase-shift data have been also used to calculate the elastic and inelastic scattering cross sections and their angular distributions. The capture cross section was calculated from the deuteron photo-disintegration cross section in conjunction with the principle of detailed balance. The presently evaluated data give a good description of the available experimental data in general and are also in good accord with those values given in ENDF-B/VI that are available below 100 MeV.

***KEYWORDS:* neutron cross sections, hydrogen, MeV range 10-1000, generalized least-squares method, phase-shift data, total cross sections, elastic scattering, inelastic scattering, capture cross sections, photon production**

I. Introduction

The interaction cross section of hydrogen with neutrons is one of the most important quantities in many fields of basic physics and nuclear technologies. First of all, the elastic *n-p* scattering cross section is the standard reference for many nuclear measurements[1]. From this point of view, information on the uncertainty of the cross section data is required strongly. On the other hand, knowledge on the *n-p* scattering provides an important insight into the nuclear force, study of which has been a main subject of the nuclear and particle physics[2]-[6]. The *n-p* scattering cross section is important as an input parameter to many programs based on microscopic simulations[7][8] as well as for the understanding of the effective inter-nucleon interaction in nuclear matter[9]. From application points of view, the neutron cross sections of hydrogen are of crucial importance because hydrogen is contained in many structural and shielding materials of fission reactors, fusion reactors and high energy accelerator facilities.

In spite of its importance, however, the *n-p* cross section is not available in an evaluated form above 20 MeV except for the Los Alamos evaluation (adopted in ENDF/B-VI) which covers an energy region below 100 MeV[10]. However, the maximum energy of 100 MeV given in ENDF/B-VI is not sufficient for many practical applications. The purpose of this work is therefore to give evaluated cross section values for the *n-p* interaction in the energy region from 20 MeV to 1 GeV as a part of evaluation of JENDL High Energy File[11]. Below 20 MeV, the data stored in JENDL-3.2[12][13], for example, are available.

The evaluation has been carried out mainly based on experimental information with the aid of the generalized least-squares method and the phase-shift data[14][15]. Evaluated values of the following quantities have been obtained: the total cross section, elastic scattering cross section (including angular distribution), inelastic (pion production) cross section (including angular distribution), capture cross section, covariance matrix of evaluated total cross section and photon production cross section. In the following, the method and results of the evaluation will be described.

II. Total Cross Section

There are sufficient data on the total cross section of hydrogen below several hundred MeV. Therefore, the total cross section was evaluated with the generalized least-squares method which utilizes the full covariance information. The least-squares analysis gave the evaluated cross section and its covariance information. This analysis, however, was restricted mainly below 800 MeV

* *Tokai-mura, Naka-gun, Ibaraki-ken 319-11.*
** *Minamisuna, Koto-ku, Tokyo 136.*
† Corresponding author, Tel. +81-29-282-5483, Fax +81-29-282-6122, E-mail: chiba@cracker.tokai.jaeri.go.jp

above which the experimental data are considerably scarce. On the other hand, Arndt *et al.*[14][15] have published a phase-shift data based on the *p-p* and *n-p* cross sections up to 1.1 GeV. In the present evaluation, the total, elastic and inelastic scattering cross sections were also calculated from the phase-shift data. The evaluated data were finally obtained by combining the results of both the generalized least-squares method and the calculation based on the phase-shift data.

1. Generalized Least-Squares Analysis

The total cross section was evaluated firstly by taking account of the available experimental data. The generalized least-squares method was employed which gave not only the cross section values but also the covariance matrix of the evaluated results because such information is crucially important for many applications, especially if the *n-p* cross section is to be used as the standard reference.

A review on the status of experimental data before 1957 is given in Ref.(16). In such old days when there was no intense source of high energy neutrons, the *n-p* cross section was obtained often by subtracting the H-*p* cross section from that of the D-*p* reaction on the basis of the Glauber approximation[17]. This might be a good approximation for very high energies (E>500 MeV) although this approach will introduce a certain bias in a lower energy region. In the present analysis, therefore, only those data reported after 1957, where the neutron cross sections have been measured directly[18]-[28], are adopted. By using these neutron data alone, there are enough data points below 800 MeV to carry out the least-squares analysis.

The list of the experimental data adopted in the present analysis is given in **Table 1**. In this table also the magnitude of the systematic errors contained in these data is shown. These systematic errors were obtained from the information given in the literature. The main sources of the systematic errors are the sample thickness, impurities and flux normalization between sample-in and sample-out runs. Among these data, those measured by Larson *et al.*[25] and Lisowski *et al.*[26] form the main base for the present analysis because they have a substantial number of data points and span wide energy ranges. Even though they are based on "white" neutron sources, it is not likely that a large "systematic" error is hidden in these data from the accuracy achieved by the current measurement techniques. However, we had to estimate the systematic error of the data of Larson *et al.* because no clear explanation on this quantity is given in the literature. The data of Blair *et al.*[24] are smaller than those of Lisowski *et al.* in the energy region from 100 to 130 MeV, showing a possibility of some hidden systematic error in the former data. This has been also pointed out by Bol *et al.*[28] and Measday *et al.*[21] Therefore, the data of Blair *et al.* have been omitted from the present analysis. Similarly, the data of Kazarinov *et al.*[19] above 700 MeV have been omitted because the error and scatter of the data are considerably large in this energy region.

Table 1 Experimental database used in the GMA analysis

Author	Energy range (MeV)	Systematic error (%)
Peterson *et al.*[18]	17.8 - 29.0	0.5
Kazarinov *et al.*[19]	100 - 1,260	1
Groce *et al.*[20]	19.6 - 28.0	1.14
Measday *et al.*[21]	88.2 - 150.0	1
Brady *et al.*[22]	24.6 - 59.4	0.3
Davis *et al.*[23]	1.5 - 27.5	0.2
Larson *et al.*[25]	0.5 - 60	1.5
Lisowski *et al.*[26]	39 - 793	0.2
Keeler *et al.*[27]	212 - 495	0.8
Bol *et al.*[28]	26.9 - 72.5	0.2

In the present evaluation, the GMA code system[29] was used for the generalized least-squares analysis of the data mentioned above. The flow chart of the GMA code system is given in **Fig. 1**. The experimental data were retrieved from NESTOR-2 data base[30], and the format is converted by the EXPTOGMA program[32]. At the same time, the prior data have been generated by NDES[30][31], and both data were put into the DATGMA code[29] which generates the data at specified energy grids and assigns the systematic errors determined as Table 1. The prior data were used only as the "shape" data in order to shift the various data to the desired energy grids. Then, the GMA code[29] performs the generalized least-squares analysis. Because of the poor data base, the total cross section was assumed to be constant above 800 MeV, as suggested by the data of Pantuev *et al.*[33]. The result is again fed into NDES in order to eliminate unphysical fluctuation of the cross

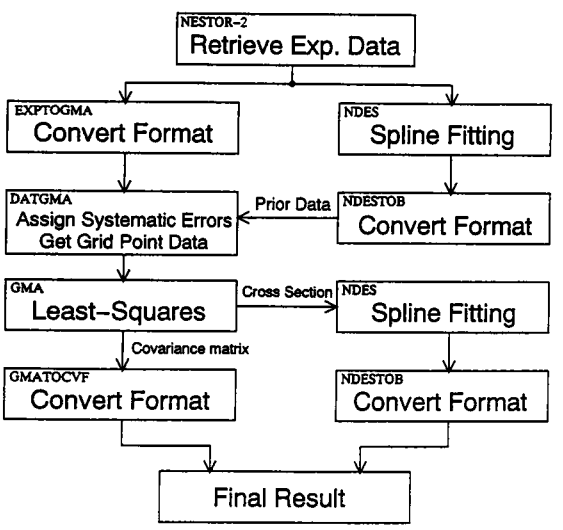

Fig. 1 Flow chart of the generalized-least-squares evaluation scheme adopted in the present work

section by spline fitting. On the other hand, the covariance information is converted to ENDF-6 format by the GMATOCVF program[32].

2. Calculation from the Phase-Shift Data

The differential elastic scattering cross section is written in the following way in partial wave representation by using the scattering amplitudes (M)[34];

$$\begin{aligned}\frac{d\sigma^{el}}{d\Omega} &= \frac{1}{4}[|M_{ss}(\theta)|^2 + |M_{00}(\theta)|^2] \\ &+\frac{1}{2}[|M_{01}(\theta)|^2 \\ &+|M_{11}(\theta)|^2 + |M_{10}(\theta)|^2 \\ &+|M_{1-1}(\theta)|^2], \end{aligned} \tag{1}$$

where the subscripts denote the z-component of the total spin in the initial and final states, *e.g.*, M_{ss} and M_{10} stand for the scattering amplitudes from the spin singlet (s) to singlet state, and s_z=1 to 0 in the spin-triplet state, respectively. The scattering amplitudes are expressed in terms of the phase-shift (δ), inelasticity (η) and mixing parameter (ϵ) as

$$M_{ss}(\theta) = \sum_l (2l+1)h_l P_l(\cos\theta) \tag{2}$$

for the singlet state, and

$$\begin{aligned} M_{11}(\theta) = \sum_l \frac{1}{2}\big[&(l+2)h_{l,l+1} + (2l+1)h_{l,l} \\ &+(l-1)h_{l,l-1} - \sqrt{(l+1)(l+2)}h^{l+1} \\ &-\sqrt{(l-1)l}h^{l-1}\big]P_l(\cos\theta), \end{aligned} \tag{3a}$$

$$\begin{aligned} M_{00}(\theta) = \sum_l \big[&(l+1)h_{l,l+1} + lh_{l,l-1} \\ &+\sqrt{(l+1)(l+2)}h^{l+1} + \sqrt{(l-1)l}h^{l-1}\big] \\ &\cdot P_l(\cos\theta), \end{aligned} \tag{3b}$$

$$\begin{aligned} M_{01}(\theta) = \sum_l \frac{1}{\sqrt{2}}\Bigg[&-\frac{l+2}{l+1}h_{l,l+1} + \frac{2l+1}{l(l+1)}h_{l,l} \\ &+\frac{l-1}{l}h_{l,l-1} + \sqrt{\frac{l+2}{l+1}}h^{l+1} \\ &- \sqrt{\frac{l-1}{l}}h^{l-1}\Bigg] P_l^1(\cos\theta), \end{aligned} \tag{3c}$$

$$\begin{aligned} M_{10}(\theta) = \sum_l \frac{1}{\sqrt{2}}\Bigg[&h_{l,l+1} - h_{l,l-1} + \sqrt{\frac{l+2}{l+1}}h^{l+1} \\ &- \sqrt{\frac{l-1}{l}}h^{l-1}\Bigg] P_l^1(\cos\theta), \end{aligned} \tag{3d}$$

$$\begin{aligned} M_{1-1}(\theta) = \sum_l \frac{1}{2}\Bigg[&\frac{1}{l+1}h_{l,l+1} - \frac{2l+1}{l(l+1)}h_{l,l} + \frac{1}{l}h_{l,l-1} \\ &- \sqrt{\frac{1}{(l+1)(l+2)}}h^{l+1} - \sqrt{\frac{1}{l(l-1)}}h^{l-1}\Bigg] \\ &\cdot P_l^2(\cos\theta) \end{aligned} \tag{3e}$$

for the triplet states, where

$$h_l = \frac{1}{2ik}(\eta_l e^{2i\delta_l} - 1), \tag{4a}$$

$$h_{l,l} = \frac{1}{2ik}(\eta_{l,l} e^{2i\delta_{l,l}} - 1), \tag{4b}$$

$$h_{l,J} = \frac{1}{2ik}[\eta_{l,J}\cos(2\epsilon_J)e^{2i\delta_{l,J}} - 1], \tag{4c}$$

and

$$h^J = \frac{1}{2k}\sin(2\epsilon_J)e^{i(\delta_{J-1,J}+\delta_{J+1,J})}. \tag{4d}$$

The symbols k, l and J denote the wave number of the relative motion, orbital angular momentum and total spin, respectively. The $P_l(\cos\theta)$ and $P_l^m(\cos\theta)$ stand for the Legendre polynomials and associated Legendre functions of rank m, respectively, and the variable θ refers to the c.m. scattering angle. The total cross section is obtained from the optical theorem as follows:

$$\begin{aligned}\sigma^{\text{total}} &= \frac{4\pi}{k}Im[M(0)] \\ &= \frac{\pi}{2k^2}\sum_l\Bigg\{(2l+1)[1-\eta_l\cos(2\delta_l)] \\ &+\sum_{J=l-1}^{l+1}(2J+1)[1-\eta_{l,J}\cos(2\epsilon_J)\cos(2\delta_{l,J})]\Bigg\}. \end{aligned} \tag{5}$$

The phase-shift parameters were primarily obtained from the work of Arndt *et al.*[14], SM86. For those energies at which the parameters are not given, they were obtained by interpolation of Arndt's data. For the i-wave parameters, however, information thus obtained was ambiguous. Therefore it was supplemented by the older work[15]. The phase-shift parameters given in Refs.(14) and (15) were converted[15] to be used in Eqs.(4a)-(4d) as

$$\eta = \left[\frac{1+K^2-2K_i}{1+K^2+2K_i}\right]^{1/2}, \tag{6a}$$

and

$$\delta = \frac{1}{2}\tan^{-1}\frac{2K_r}{1-K^2}, \tag{6b}$$

where $K_i = \tan^2(\rho_A)$, (7a)

$K_r = \tan^2(\delta_A)$, (7b)

$K^2 = K_r^2 + K_i^2$ (7c)

for uncoupled waves, *i.e.*, the singlet and triplet uncoupled ($^3P_1$, $^3D_2$, $\cdots$) waves. The subscript A denotes those quantities are given by Arndt *et al.*[14][15] For spin-coupled waves the following equations were used:

$$\eta_\mp = \sqrt{\frac{|s_\mp|^2}{1-|s_0|^2}}, \tag{8a}$$

$$\delta_\mp = \frac{1}{2}\tan^{-1}\left[\frac{Im(s_\mp)}{Re(s_\mp)}\right], \tag{8b}$$

$$\epsilon = \frac{1}{2}\sin^{-1}\sqrt{|s_0|^2}, \tag{8c}$$

where $s_{\mp} = [1 + d_k \mp i(K_+ - K_-)]/D_k$, (9a)

$$s_0 = 2iK_0/D_k, \quad (9b)$$

$$D_k = 1 - d_k - i(K_+ + K_-), \quad (9c)$$

$$d_k = K_+K_- - K_0^{-2}, \quad (9d)$$

$$K_\pm = \frac{\sin(\delta_{+A} + \delta_{-A}) \pm \cos(2\epsilon_A)\sin(\delta_{+A} - \delta_{-A})}{\cos(\delta_{+A} + \delta_{-A}) + \cos(2\epsilon_A)\cos(\delta_{+A} - \delta_{-A})} + i\tan^2(\rho_{\pm A}), \quad (9e)$$

$$K_0 = \frac{\sin(2\epsilon_A)}{\cos(\delta_{+A} + \delta_{-A}) + \cos(2\epsilon_A)\cos(\delta_{+A} - \delta_{-A})} + i\tan(\delta_{-A})\tan(\delta_{+A})\cos(\phi_A). \quad (9f)$$

The subscript $\pm$ stands for a partial wave state ${}^3l_J$ where l=$J\pm1$.

3. Evaluated Total Cross Section of Hydrogen

The total cross sections obtained from the GMA analysis and the phase-shift data are compared in **Fig. 2**. The neutron energy in this and the subsequent figures and the tables is given in the laboratory frame. In general below several hundred MeV, the two results are in good agreement within the uncertainty obtained from the GMA analysis. Above around 700 MeV, however, the result calculated from the phase-shift data is slightly smaller than that of the GMA analysis. The experimental data seem to prefer the lower cross section values. In the present evaluation, therefore, result of the GMA analysis was adopted below 500 MeV, and was connected smoothly to the data calculated from the phase-shift above 500 MeV. The uncertainty of the presently evaluated total cross section above 800 MeV corresponding to the phase-shift data was subjectively estimated to be 2%, otherwise the covariance matrix obtained from the GMA analysis was adopted.

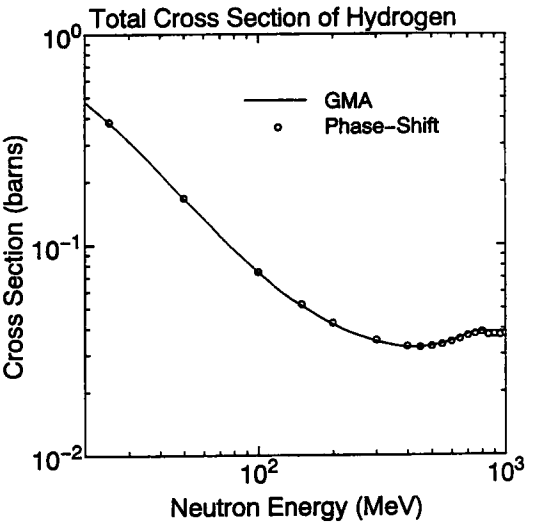

Fig. 2 Comparison of the total cross sections obtained from the GMA analysis and phase-shift data
In this and the subsequent figures, the neutron energy is given in the laboratory frame.

In **Fig. 3**, the evaluated total cross section of hydrogen is compared with experimental data and evaluated values given in ENDF/B-VI. The agreement among the present result, ENDF/B-VI and the experimental data is excellent. The error-correlation matrix of the presently evaluated data is displayed in **Fig. 4**. The present result has a correlation of medium strength below 800 MeV. This is due to the existence of Lisowski *et al.*'s data which extend from 40 MeV up to this energy. The values of the total cross section (σ^{total}) and its uncertainty ($\Delta\sigma^{\text{total}}$) are listed in **Table 2** at selected energies as well as the

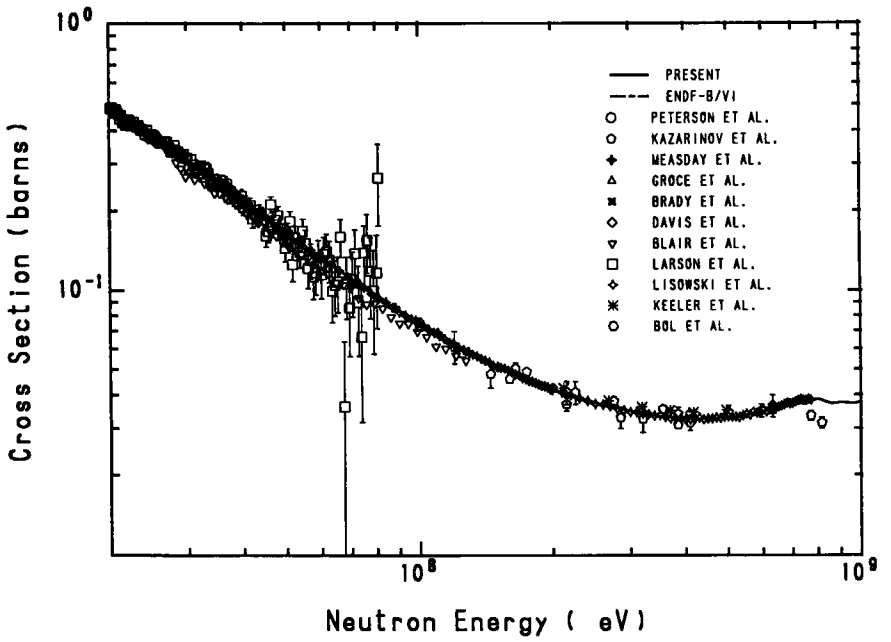

Fig. 3 Total neutron cross section of hydrogen

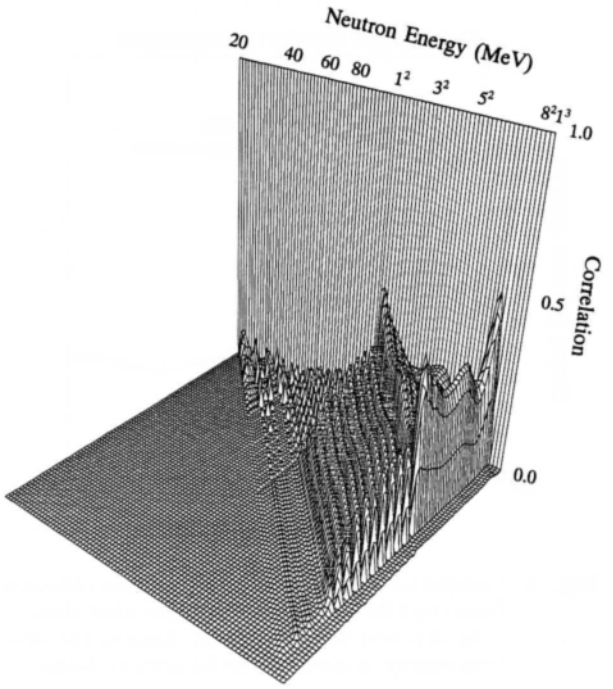

Fig. 4 Error-correlation matrix of the evaluated neutron total cross section of hydrogen
The sign such as 1^3 stands for 10^3 MeV.

Table 2 The evaluated n-p cross sections and uncertainty at selected energies

Energy (MeV)	σ^{total} (barn)	$\Delta\sigma^{\text{total}}$ (%)	σ^{el} (barn)	σ^{in} (barn)	σ^{cap} (barn)
20	0.4801	0.43	0.4801		2.551^{-5}
30	0.3109	1.60	0.3109		2.231^{-5}
40	0.2195	0.71	0.2195		1.967^{-5}
50	0.1666	0.91	0.1666		1.782^{-5}
60	0.1342	0.58	0.1342		1.633^{-5}
70	0.1112	0.55	0.1112		1.514^{-5}
80	0.09502	2.00	0.09501		1.415^{-5}
90	0.08343	0.49	0.08342		1.333^{-5}
100	0.07442	0.28	0.07441		1.266^{-5}
200	0.04205	0.31	0.04204		9.289^{-6}
300	0.03491	0.37	0.03486	4.599^{-5}	7.683^{-6}
400	0.03269	0.36	0.03172	9.721^{-4}	6.717^{-6}
500	0.03299	0.34	0.03011	2.872^{-3}	6.055^{-6}
600	0.03467	0.44	0.02820	6.468^{-3}	5.568^{-6}
700	0.03709	0.26	0.02729	9.792^{-3}	5.190^{-6}
800	0.03871	2.00	0.02741	1.129^{-2}	4.886^{-6}
900	0.03752	2.00	0.02542	1.209^{-2}	4.636^{-6}
1,000	0.03768	2.00	0.02525	1.243^{-2}	4.425^{-6}

The symbol a^b stands for $a\times10^b$.

evaluated elastic (σ^{el}), inelastic (σ^{in}) and capture (σ^{cap}) cross sections which will be explained below.

III. Capture Cross Section

There is not enough information on the H(n,γ)D reaction cross sections above 20 MeV. In the present evaluation, this cross section was calculated from the D(γ,n)H reaction cross section by use of the principle of detailed balance. Below 140 MeV, the D(γ,n)H cross section was taken from the evaluation of Murata[63]. Above 140 MeV, theoretical D(γ,n)H cross section of Feshbach and Schwinger[64] was adopted which leads to the following formula of Horsley[65]:

$$\sigma^{\text{cap}}[\text{mb}] = \frac{0.0528}{\sqrt{E}} \cdot \frac{(1+0.2444E)(1+0.0103E)^2}{1+7.46E+0.158E^2} + \frac{0.143\sqrt{E}}{4.46+E}, \tag{10}$$

where E is the laboratory neutron energy in MeV. This formula, however, gave slightly higher values than those calculated from the inverse reaction cross section of Murata. Therefore, Eq.(10) was renormalized at 140 MeV so as to give a smooth cross section curve below and above this energy. The result is compared with experimental data[66]-[69] and ENDF/B-VI in **Fig. 5**.

The capture cross section was also adopted as the production cross section of 2.2-MeV γ-ray.

IV. Elastic and Inelastic Scattering Cross Sections

The evaluation of inelastic scattering cross section was performed based on the phase-shift data of Arndt *et al.*[14][15] as follows:

$$\sigma^{\text{in}} = \frac{\pi}{4k^2}\sum_l \Bigg\{ (2l+1)(1-\eta_l^2) + \sum_{J=l-1}^{l+1}(2J+1)[1-\eta_{l,J}^2\cos^2(2\epsilon_J)] - \sum_{J=l-1,J\neq l}^{l+1}(2J+1)\sin^2(2\epsilon_J) \Bigg\}. \tag{11}$$

The angle-integrated inelastic scattering cross section is given in **Fig. 6** together with experimental data which were graphically obtained from Ref.(62). An error of

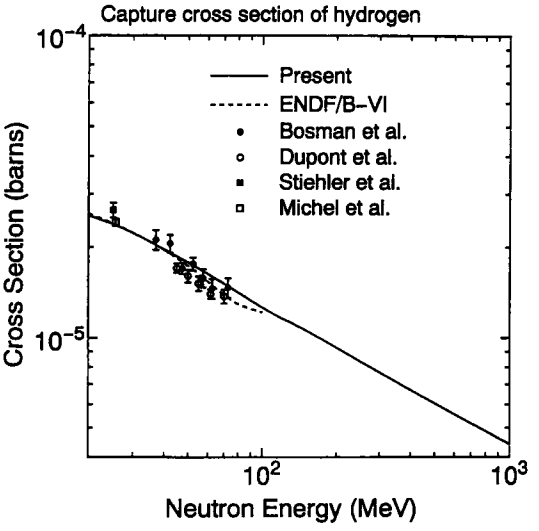

Fig. 5 Neutron capture cross section of hydrogen

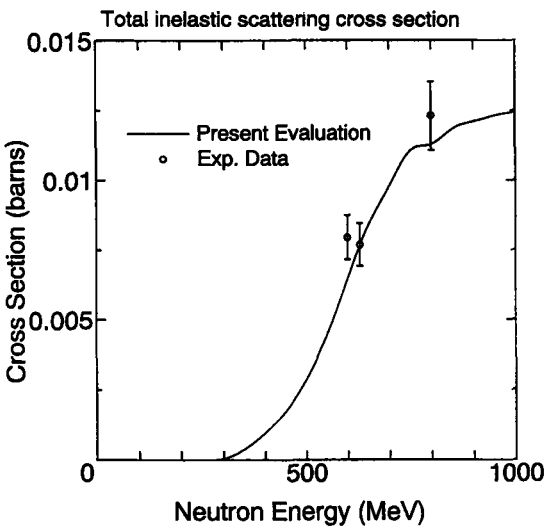

Fig. 6 Total inelastic scattering cross section of hydrogen

10% was assigned to the experimental data points for purpose of graphical comparison. The evaluated data reproduce the genereal trend of the experimentally obtained values.

The elastic scattering cross section was calculated by subtracting the inelastic and capture cross sections from the evaluated total cross section. The evaluated elastic scattering cross section is compared in **Fig. 7** with experimental data and ENDF/B-VI. The experimental data were obtained by fitting the Legendre polynomials of the form

$$\frac{d\sigma}{d\Omega} = \frac{\sigma^{\mathrm{el}}}{4\pi}\left[1 + \sum_{l=1}(2l+1)a_l P_l(\cos\theta)\right] \tag{12}$$

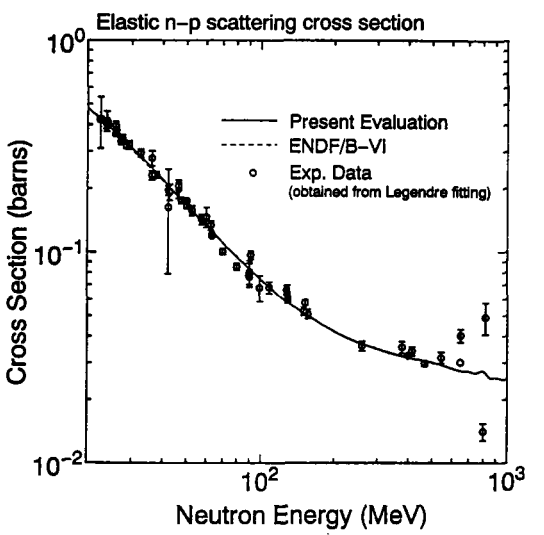

Fig. 7 Elastic neutron scattering cross section of hydrogen
The experimental points (denoted by circles) have been obtained by the Legendre fitting of available angular distribution data[35]-[61].

to experimental angular distribution data[35]-[61]. The present evaluation gives a good reproduction of the experimentally deduced values in the whole energy region. Below 100 MeV, ENDF-B/VI gives essentially same values as the present results. The present results are also consistent with the data calculated from the phase-shift data according to the following formula:

$$\begin{aligned}\sigma^{\mathrm{el}} = \frac{\pi}{4k^2}\sum_l \Bigg\{ & (2l+1)[1+\eta_l^2 - 2\eta_l\cos(2\delta_l)] \\ & + \sum_{J=l-1}^{l+1}(2J+1)[1+\eta_{l,J}^2\cos^2(2\epsilon_J) \\ & -2\eta_{l,J}\cos(2\epsilon_J)\cos(2\delta_{l,J})] \\ & + \sum_{J=l-1,J\neq l}^{l+1}(2J+1)\sin^2(2\epsilon_J)\Bigg\}.\end{aligned} \tag{13}$$

The differential elastic scattering cross section was calculated based on the phase-shift data[14][15]. Instead of calculating the cross sections, however, the Legendre expansion coefficients (a_l) are calculated directly from the phase-shift data up to l=12. The result is compared in **Fig. 8** with the data deduced by the Legendre fitting of the experimental data. The present evaluation, shown as solid lines, well reproduces the data up to around 400 MeV. Above this energy, the data (mainly by Shepard *et al.*[54]) deviate toward higher values systematically. We thus tried to fit smooth curves to these data for a_1 to a_5 as shown by the broken curves in Fig. 8. It turned out, however, that the angular distributions calculated by using the broken curves (and the solid curves for a_6 and higher partial waves) became negative at backward angles or gave unphysical oscillations at some energy regions. Because of this reason, we decided to accept the result calculated from the phase-shift data (the solid lines).

The evaluated angular distributions of *n-p* elastic scattering are compared with experimental data[44][47][54][57][59]-[61] at several incident energies in **Fig. 9**. The present evaluation reproduces the measured values quite well below 400 MeV. Above this energy, however, agreement becomes slightly worse.

The differential inelastic scattering cross section is calculated by substituting the following expressions of the h-coefficients into Eqs.(1) to (3):

$$h_l^{\mathrm{in}} = \frac{1}{2k}\sqrt{1-\eta_l^2}, \tag{14a}$$

$$h_{l,l}^{\mathrm{in}} = \frac{1}{2k}\sqrt{1-\eta_{l,l}^2}, \tag{14b}$$

$$h_{l,J}^{\mathrm{in}} = \frac{1}{2k}\sqrt{1-\eta_{l,J}^2}, \tag{14c}$$

$$h^{J\mathrm{in}} = 0. \tag{14d}$$

These expressions were derived on the assumption that the angle-integrated inelastic scattering cross section becomes identical with the previous one(see Eq.(11)). The

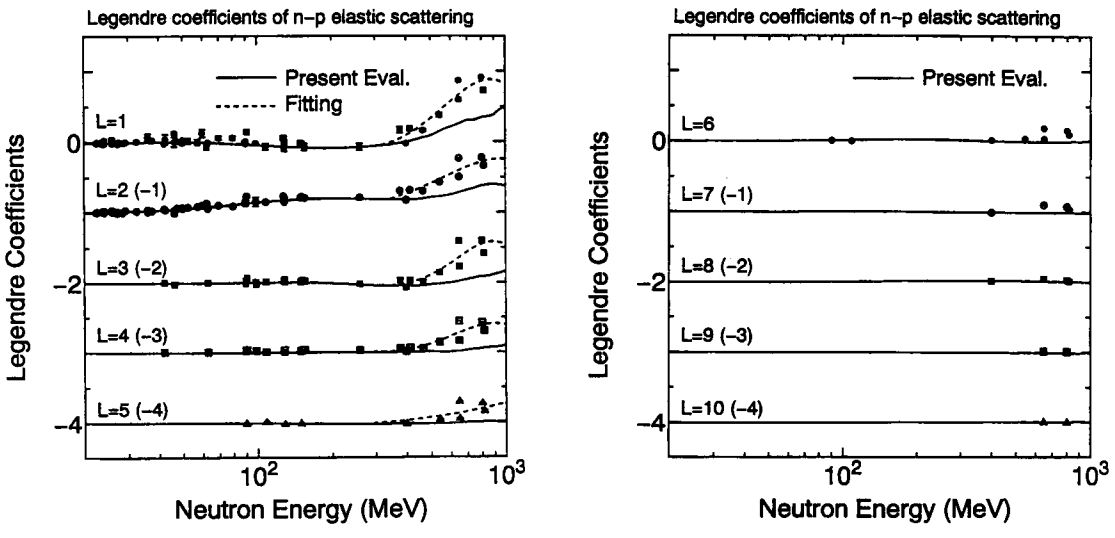

Fig. 8 Legendre coefficients of *n-p* elastic scattering angular distribution
The data have been shifted by the amount denoted in the parentheses. The experimental points (denoted by symbols) have been obtained by the Legendre fitting of available angular distribution data[35)-61)].

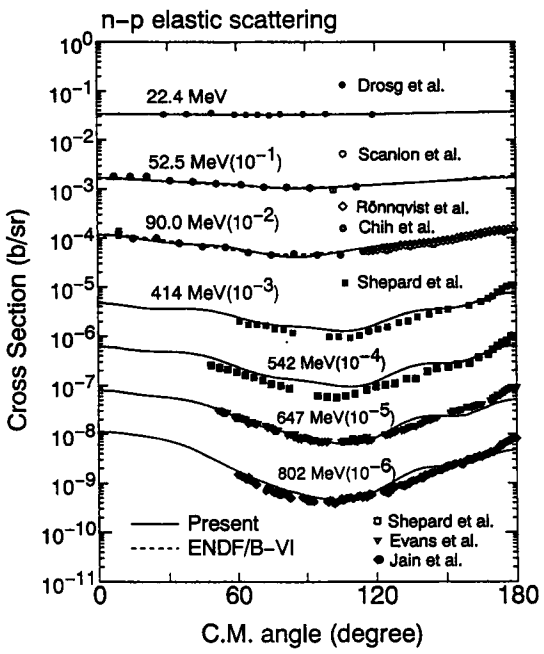

Fig. 9 Angular distributions of *n-p* elastic scattering
The data have been multipled by the factors denoted in the parenthese.

angular distributions of the inelastic scattering are also expressed in the form of Legendre expansion.

V. Concluding Remarks

The neutron cross sections of hydrogen have been evaluated in the energy region from 20 MeV to 1 GeV. The total cross section was evaluated mainly based on available experimental data by employing the generalized least-squares method and the phase-shift data of Arndt *et al.* The full covariance information of the evaluated total cross section was also obtained from the least-squares analysis. Other cross sections, *i.e.*, the elastic and inelastic scattering including their angular distributions are evaluated based on the phase-shift data. The capture cross section was evaluated from the inverse reaction cross section through the principle of detailed balance. The presently evaluated values are compiled in ENDF-6 format as a part of JENDL High Energy File.

It must be noted that the phase-shift data used in this work is not the most up-to-date ones nowadays. Arndt *et al.* has already extended the nucleon-nucleon phase-shift analysis up to 1.6 GeV[70] which was not available when the present work was started. However, the new extention has been performed only for isovector partial-waves, which is enough to calculate the *p-p* scattering cross sections, but not enough to determine the necessary matrix elements for the *n-p* system. Moreover, the new (1992) and old (1987) solutions well agree with each other below 1 GeV. This is the reason why we decided not to make the re-evaluation by using the new Arndt's phase-shift data.

Acknowledgments

The authors are grateful to a help and comments from Dr. R.A. Arndt on the phase-shift calculations.

—References—

(1) *e.g.*, Nuclear standard reference data, *Proc. Advisory Group Meeting on Nuclear Standard Reference Data, IAEA-TECDOC*-335, (1984).
(2) Yukawa, H.: *Proc. Phys. Math. Soc. Jpn.*, **17**, 48 (1935).
(3) Hamada, T., Johnston, I.: *Nucl. Phys.*, **34**, 382 (1962).
(4) Reid, Jr. R.V.: *Ann. Phys.* (NY), **50**, 411 (1968).

(5) Lacombe M., Loiseau, B., Richard, J.M., Vinh Mau, R., Côté, J., Pirès, P., de Tourreil, R.: *Phys. Rev.*, **C21**, 861 (1980).
(6) Machleidt, R.: *Adv. Nucl. Phys.*, **19**, 189 (1989).
(7) Bertsch, G.F., Das Gupta, S.: *Phys. Rep.*, **160**, 189 (1988).
(8) Bertini, H.W.: Monte Carlo calculation on intranuclear cascades, *ORNL*-3383, (1963).
(9) Jeukenne, J.P., Lejeune, A., Mahaux, C.: *Phys. Rev.*, **C15**, 10 (1977).
(10) Young, P.G., Arthur, E.D., Bozoian, M., England, T.R., Hale, G.M., LaBauve, R.J., Little, R.C., Macfarlane, R.E., Madland, D.G., Perrey, R.T., Wilson, W.B.: Transport data libraries for incident proton and neutron energies to 100 MeV, *LA*-11753-*MS*, (1989).
(11) Fukahori, T., Chiba, S., Kikuchi, Y., Kawai, M., Kishida, N.: Status of nuclear data evaluation for JENDL high energy file, *Proc. Int. Conf. on Nuclear Data for Science and Technology, May 9-13, 1994, Gatlinburg, U.S.A.*, World Scientific, p.765 (1995).
(12) Shibata, K., Nakagawa, T., Asami, T., Fukahori, T., Narita, T., Chiba, S., Mizumoto, M., Hasegawa, A., Kikuchi, Y., Nakajima, Y., Igarashi, S.: Japanese evaluated nuclear data library, Version-3, JENDL-3, *JAERI* 1319, (1990).
(13) Nakagawa, T., Shibata, K., Chiba, S., Fukahori, T., Nakajima, Y., Kikuchi., Y., Kawano, T., Kanda, Y., Ohsawa, T., Matsunobu, H., Kawai, M., Zukeran, A., Watanabe, T., Igarasi, S., Kosako, K., Asami, T.: *J. Nucl. Sci. Technol.*, **32**, 1259 (1995).
(14) Arndt, R.A., Hyslop III, J.S., Roper, L.D.: *Phys. Rev.*, **D35**, 128 (1987).
(15) Arndt, R.A., Roper, L.D., Bryan, R.A., Clark, R.B., VerWest, B.J., Singnell, P.: *Phys. Rev.*, **D28**, 97 (1983).
(16) Hess, W.N.: *Rev. Mod. Phys.*, **30**, 368 (1958).
(17) Chen, F.F., Leavitt, C.P., Shapiro, A.M.: *Phys. Rev.*, **103**, 211 (1956).
(18) Peterson, J.M., Bratenahl, A., Stoering, J.P.: *ibid.*, **120**, 521 (1960).
(19) Kazarinov, J.M., Satarov, V.I., Simonov, J.N.: *Sov. J. Nucl. Phys.*, **1**, 191 (1965).
(20) Groce, D.E., Sowerby, B.D.: *Nucl. Phys.*, **83**, 199 (1966).
(21) Measday, D.F., Palmieri, J.N.: *ibid.*, **85**, 142 (1966).
(22) Brady, F.P., Knox, W.J., Jungerman, J.A., McGie, M.R., Walraven, R.L.: *Phys. Rev. Lett.*, **25**, 1628 (1970).
(23) Davis, J.C., Barschall, H.H.: *Phys. Rev.*, **C3**, 1798 (1971).
(24) Blair, I.M., Asbury, D.A., Edgington, J.: Few nucleon studies on the Synchrocyclotron, *Proc. Int. Conf. in Interactions of Neutrons With Nuclei, Lowerll, U.S.A., 6-9 July 1976*, p.1238 (1976).
(25) Larson, D.C., Harvey, J.A., Hill, N.W.: Neutron total cross sections of hydrogen, carbon, oxygen and iron from 500 keV to 60 MeV, *Proc. Int. Conf. on Nuclear Cross Sections for Technology, Knoxvill, 22-26 Oct., 1979*, p.34 (1980).
(26) Lisowski, P.W., Shamu, R.E., Auchampaugh, G.F., King, N.S.P., Moore, M.S., Morgen, G.L., Singleton, T.S.: *Phys. Rev. Lett.*, **49**, 255 (1982).
(27) Keeler, R.K., Dubios, R., Auld, E.G., Axen, D.A., Comyn, M., Ludgate, G., Robertson, L.P., Richardson, J.R., Bugg, D.V., Eddington, J.A., Gibson, W.R., Clouch, A.S., Stewart, N.M., Dieterle, B.: *Nucl. Phys.*, **A377**, 529 (1982).
(28) Bol, A., Devescovi, P., Leleux, P., Lipnik P., Macq, P., Meulders, J.P.: *Phys. Rev.*, **C32**, 623 (1985).
(29) Poenitz, W.P.: Data interpretation, objective evaluation procedures and mathematical techniques for the evaluation of energy-dependent ratio, shape and cross section data, *Proc. Conf. in Nuclear Data Evaluation Methods and Procedures, BNL-NCS*-51363, p.249 (1981).
(30) Nakagawa, T.: *J. At. Energy Soc. Jpn.*, **22**, 559 (1980), [in Japanese].
(31) Fukahori, T.: Program NDESTOB, unpublished.
(32) Chiba, S.: Programs EXPTOGMA and GMATOCVF, unpublished.
(33) Pantuev, V.S., Khachaturjan, M.K., Chuvilo, I.V.: *Sov. J. Nucl. Phys.*, **1**, 93 (1965).
(34) Hoshizaki, N.: *Prog. Theor. Phys. Suppl.*, **42**, 107 (1968).
(35) Hadley, J., Kelly, E., Leith, C., Segere, E., Wiegand, C., York, H.: *Phys. Rev.*, **75**, 351 (1949).
(36) Kelley, E., Leith, C., Segre, E., Weigand, C.: *ibid.*, **79**, 96 (1950).
(37) Fox, R.H.: Neutron-proton scattering at 90 MeV, *UCRL*-867, (1950).
(38) Wallance, R.: *Phys. Rev.*, **81**, 493 (1951).
(39) Randle, T.C., Taylor, A.E., Wood, E.: *Proc. Phys. Soc. (London)*, **A218**, 392 (1952).
(40) Hartzler, A.J., Siegel, R.T., Opitz, W.: *Phys. Rev.*, **95**, 591 (1954).
(41) Thresher, J.J., Voss, R.G.P., Wilson, R.: *Proc. Phys. Soc. (London)*, **A229**, 492 (1954).
(42) Stahl, R.H., Ramsey, N.F.: *Phys. Rev.*, **96**, 1310 (1954).
(43) Randle, T.C., Skyrme, D.M., Snowden, M., Taylor, A.E., Uridge, F., Wood, E.: *Proc. Phys. Soc.*, **A69**, 760 (1956).
(44) Chih, C.Y., Powell, W.M.: *Phys. Rev.*, **106**, 539 (1957).
(45) Hobbie, R.K., Miller, D.: *ibid.*, **120**, 2201 (1960).
(46) Flynn, E.R., Bendt, P.J.: *ibid.*, **128**, 1268 (1962).
(47) Scanlon, J.P., Stafford, G.H., Thresher, J.J., Bowen, P.H., Langsford, A.: *Nucl. Phys.*, **41**, 401 (1963).
(48) Measday, D.F.: *Phys. Rev.*, **142**, 584 (1966).
(49) Romero, J.L., Jungerman, J.A., Brady, F.P., Knox, W.J., Ishizaki, Y.: *ibid.*, **C2**, 2134 (1970).
(50) Sartmarsh, M.J., Halbert, M.L., Bingham, C.R., Ludemann, C.A., van der Woude, A.: *n-p* elastic scattering at 60 MeV, *ORNL*-4534, (1970).
(51) Palmieri, J.N., Wolfe, J.P.: *Phys. Rev.*, **C3**, 144 (1971).
(52) Burrows, T.W.: *ibid.*, **C7**, 1306 (1973).
(53) Howared, V.J., Edington, J.A., Das Gupta, S.S., Blair, I.M., Bonner, B.E., Brady, F.P., Mcnaughton, M.W., Steward, N.M.: *Nucl. Phys.*, **A218**, 140 (1974).
(54) Shepard, P.F., Devlin, T.J., Mischke, R.E., Solomon, J.: *Phys. Rev.*, **D10**, 2735 (1974).
(55) Bersbach, A.J., Mischke, R.E., Devlin, T.J.: *ibid.*, **D13**, 535 (1976).
(56) Montgomery, T.C., Brady, F.P., Bonner, B.E., Broste, W.B., McNaughton, M.W.: *ibid.*, **C16**, 49 (1977).
(57) Drosg, M.: Interaction of fast neutrons with ^{4}He, ^{3}He and ^{1}H, *LA*-7269-*MS*, (1978).
(58) King, N.S.P., Reber, J.D., Romero, J.L., Fitzgerald, D.H., Ullmann, J.L., Subramanian, T.S., Brady, F.P.: *Phys. Rev.*, **C21**, 1185 (1980).
(59) Evans, M.L., Glass, G., Hiebert, J.C., Jain, M., Kenefick, R.A., Northcliffe, L.C., Bonner, B.E., Simmons, J.E., Bjork, C.W., Riley, P.J., Bryant, H.C., Cassapakis, C.G., Dieterle, B., Leavitt, C.P., Wolfe, D.M., Werren, D.W.: *ibid.*, **C26**, 2525 (1982).
(60) Jain, M., Evans, M.L., Glass, G., Hielbert, J.C., Kenefick, R.A., Northcliffe, L.C., Bonner, B.E., Simmons, J.E., Bjork, C.W., Riley, P.J., Bryant, H.C., Cassapakis, C.G., Dieterle, B., Leavitt, C.P., Wolfe, D.M., Warren, D.W.: *ibid.*, **C30**, 568 (1984).

(61) Rönnqvist, T., Condé, H., Olsson, N., Zorro, R., Blomgren, J., Tibell, G., Jonsson, O., Nilsson, L., Renberg, P.-U., van der Werf, S.Y.: *ibid.*, **C45**, 496 (1992).
(62) Lehar, F.: Status of (n-p) data in the enegy region below 1100 MeV, *Proc. Specialists' Meeting on Neutron Cross Section Standards for the Energy Region above 20 MeV, Uppsala, Sweden 21-23 May 1991, NEANDC-305* 'U', p.26 (1991).
(63) Murata, T.: Evaluation of the $D(\gamma, n)$ reaction cross section, *JAERI-M* 94-019, p.330 (1994).
(64) Feshbach, H., Schwinger, J.: *Phys. Rev.*, **84**, 194 (1951).
(65) Horsley, A.: *Nucl. Data*, **2**, 243 (1966).
(66) Bosman, M., Bol, A., Gilot, J.F., Leleux, P., Lipnik, P., Macq, P.: *Phys. Lett.*, **B82**, 212 (1979).
(67) Dupont, C., Leleux, P., Lipnik, P., Macq, P., Ninane, A.: *Nucl. Phys.*, **A445**, 13 (1985).
(68) Stiehler, T., Kuehn, B., Moeller, K., Moesner, J., Neubert, W., Pilz, W., Schmidt, G.: *Nucl. Instum. Methods*, **A236**, 343 (1985).
(69) Michel, P., Moeller, K., Moesner, J., Schmidt, G.: *J. Phys. G.*, **15**, 1025 (1989).
(70) Arndt, R.A., Roper, L.D., Workman, R.L., McNaughton, M.W.: *Phys. Rev.*, **D45**, 3995 (1992).